Acrylic-based resin with favorable properties for three-dimensional two-photon polymerization

Tommaso Baldacchini, Christopher N. LaFratta, and Richard A. Farrer
Eugene F. Merkert Chemistry Center, Boston College, Chestnut Hill, Massachusetts 02467

Malvin C. Teich and Bahaa E. A. Saleh
Quantum Imaging Laboratory, Department of Electrical and Computer Engineering, Boston University, Boston, Massachusetts 02215

Michael J. Naughton
Department of Physics, Boston College, Chestnut Hill, Massachusetts 02467

John T. Fourkas[a]
Eugene F. Merkert Chemistry Center, Boston College, Chestnut Hill, Massachusetts 02467

We describe an acrylic-based prepolymer resin that is ideally suited for the fabrication of three-dimensional structures with two-photon polymerization. We characterize the photochemical and photophysical properties of the photoinitiator and present representative structures that demonstrate the favorable mechanical and optical properties of the polymer. © *2004 American Institute of Physics.* [DOI: 10.1063/1.1728296]

I. INTRODUCTION

Multiphoton absorption[1–3] (MPA) is attracting increasing attention as a tool for the fabrication of three-dimensional structures[4–16] that cannot be created using standard lithographic techniques. Due to the nonlinear nature of MPA, photochemical or photophysical events can be localized within the focal volume of an ultrafast laser beam that has passed through a microscope objective. By translating the focal point of the laser relative to a sample, complex three-dimensional patterns can be created. Furthermore, if additional nonlinearity is involved in the fabrication process,[17] it is possible to create structures having features that are considerably smaller than the diffraction limit of light.

Radical photopolymerization has been the most commonly used process for fabrication via MPA. In this technique, fabrication is performed in a viscous liquid prepolymer resin that contains a photoinitiator. MPA by the photoinitiator leads to the generation of radicals that induce a polymerization chain-reaction, thereby hardening the resin locally. Once fabrication is complete, the unexposed resin can be washed away with a solvent, leaving behind the desired structure.

The materials most commonly used for multiphoton polymerization (MPP) are acrylic resins. Acrylates generally have high rates of polymerization, which makes them attractive candidates for MPP. Furthermore, a wide variety of acrylate monomers is available, making it possible to tailor the physical and chemical properties of a resin to its intended application. However, much of the previous work on MPP of acrylates has employed commercial resins with proprietary

components.[5,9] Little effort has been reported on the development of resins for MPP that have desirable properties. Here we present an acrylate resin that we have developed for MPP that has advantageous physical and chemical properties. We characterize the MPP initiation properties of the resin, and present structures that exhibit low shrinkage, high mechanical strength and hardness, and good optical quality.

II. EXPERIMENT

Our resin formulation has three components. The first component, ethoxylated(6) trimethy-lolpropane triacrylate (Sartomer), helps to reduce shrinkage upon polymerization. The second component, tris(2-hydroxyethyl)isocyanurate triacrylate (Sartomer), promotes hardness of the polymer. The final component, Lucirin TPO-L (Ciba), is an acylphosphine oxide radical photoinitiator that has a number of advantageous properties for MPP. Unlike most radical photoinitiators, Lucirin TPO-L is a liquid and has broad solubility, so it can be mixed easily into most resin formulations. Its efficient initiation of polymerization under two-photon excitation (*vide infra*) demonstrates that it has a significant two-photon absorption cross section for light with a wavelength near 800 nm.

The first step in sample preparation is placing the three components together in a test tube and agitating them for at least 2 h to ensure complete mixing of the viscous liquid. A typical formulation contains roughly equal weight percentages of the two acrylate monomers and a few weight percent of photoinitiator. Once the resin is fully mixed, a drop of it is placed inside a spacer that is on top of a microscope slide that has been treated with (3-acryloxypropyl)trimethoxysilane to promote adhesion of the final structure. The spacer is thinner than the working distance of the microscope objective used. After introduction of the resin, a cover slip is placed on top of the spacer. For one

---

[a]Author to whom correspondence should be addressed. Electronic address: fourkas@bc.edu

representative structure, a human hair was bleached and glued to the microscope slide at two spots before the resin was added (*vide infra*).

Experiments are performed with a broadly tunable, commercial Ti:sapphire laser oscillator (Coherent Mira 900-F) that produces optical pulses with a duration of ~100 fsec. The laser output is sent through a Faraday isolator, a prism dispersion compensator and a beam expander before being introduced into a commercial upright microscope (Zeiss AxioPlan2) through the reflected light port. The beam is directed through the objective and into the sample by a 90% reflective beam splitter. In order to maximize the resolution of fabricated objects, the beam diameter is considerably larger than that of the back aperture of the objective. For this reason, all powers cited herein are as measured at the sample position.

The position of the focal volume is controlled perpendicularly to the beam propagation direction with a computerized stage (Ludl BioPrecision) and along the beam propagation direction with the focusing drive of the microscope. The resolutions in these directions are 100 nm and 25 nm, respectively. Fabrication commences with the opening of a shutter in the beam path. The sample is visualized with a charge coupled device camera using transmitted white light with a filter to remove any reflected excitation light. A long-pass filter is placed in front of the white-light source to prevent any single-photon polymerization. The polymerized material has a significantly higher refractive index than does the prepolymer resin (1.5222 vs 1.4930), so that fabricated objects are readily visible. After fabrication is complete, the cover slip is removed and the unexposed resin is washed away with ethanol. All structures were coated with a thin film of gold in a sputter coater for imaging via scanning electron microscopy.

III. CHARACTERIZATION OF THE PHOTOINITIATOR

In single-photon polymerization, it is essential that the absorption path length be comparable to or larger than the thickness of the object to be polymerized so that absorption does not prevent the polymerization of the portion of the object farthest from the light source. This requirement places a significant constraint on the concentration of photoinitiator that can be used for single-photon polymerization. However, in MPP the sample is transparent at the laser wavelength, and MPA occurs only within the focal region. As a result, it is possible to use a considerably higher photoinitiator concentration in MPP. The only potentially deleterious effect that might occur at high concentrations of photoinitiator is a lowering of the damage threshold, since MPA by the photoinitiator will be the major mechanism for depositing heat at the focus of the laser beam.

To determine the optimal concentration of Lucirin TPO-L, samples were prepared with roughly equal weight percentages of ethoxylated(6) trimethylolpropane triacrylate and tris(2-hydroxyethyl)isocyanurate triacrylate and a various weight percentages of photoinitiator. The laser beam, which was tuned to 785 nm, was focused somewhere in the middle of the sample (far away from the substrate) using a
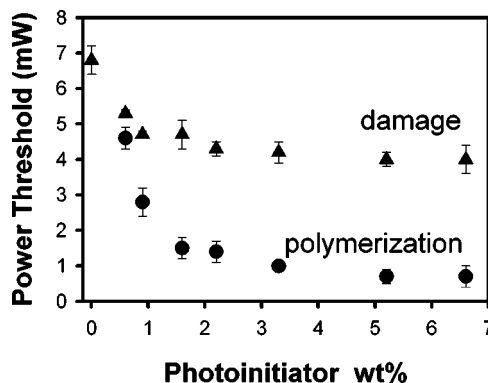

FIG. 1. Threshold powers for polymerization (●) and damage (▲) of acrylate prepolymer resin after 5 s of laser exposure as a function of photoinitiator weight percent.

40×, 1.3-NA oil-immersion objective. Different spots in the sample was exposed for 5 s each at various powers. The damage threshold $P_{th,dam}$ was defined as the minimum power at which uncontrolled polymerization took place after this exposure time. The fabrication threshold $P_{th,fab}$ was defined as the minimum power at which a polymerized spot was visible after this exposure time. Note that it is possible to fabricate spots that cannot be visualized in the microscope, so the actual fabrication threshold is considerably lower than the one measured with this technique.

Figure 1 shows the results of these experiments. It can be seen from this figure that $P_{th,fab}$ decreases rapidly with increasing photoinitiator concentration up to about 1.5 wt %, after which it decreases only slowly. By approximately 3 wt % of photoinitiator visible features can be fabricated with less than one milliwatt of power at the sample. The damage threshold $P_{th,dam}$ on the other hand, decreases slightly with increasing photoinitiator concentration until about 1 wt %, after which it remains relatively stable. Thus, an optimal dynamic range for fabrication is attained at photoinitiator concentrations of 1.5 wt % and higher. All further experiments discussed below were performed with 3 wt % of the photoinitiator, 48 wt % of ethoxylated(6) trimethylolpropane triacrylate and 49 wt % of tris(2-hydroxyethyl)isocyanurate triacrylate.

Assuming that the polymerization threshold is reached when a given concentration of radicals is attained and that a constant pulse duration and repetition rate are employed, then

$$P_{th,fab}^2(\omega)\sigma_2(\omega)\phi_2(\omega)=k, \qquad (1)$$

where $\sigma_2(\omega)$ is the two-photon absorption cross section, $\phi_2(\omega)$ is the radical quantum yield, and k is a constant. The polymerization action spectrum $A(\omega)$ is obtained by rearranging this equation:

$$A(w)\propto \frac{1}{P_{th,fab}^2(\omega)}=\frac{\sigma_2(\omega)\phi_2(\omega)}{k}. \qquad (2)$$

The two-photon radical quantum yield at frequency ω can be estimated by measuring the single-photon fluorescence quantum yield at frequency 2ω. The latter quantity was determined to be 0.006 at a wavelength of 400 nm by comparison
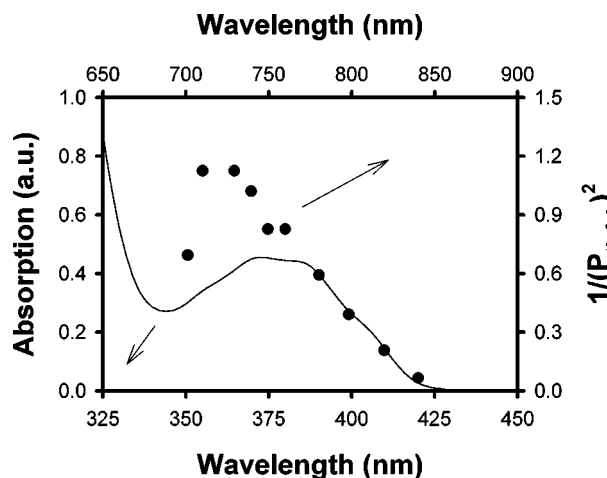
FIG. 2. Single-photon absorption spectrum (solid line) and two-photon action spectrum (circles) of the acrylate prepolymer resin.

of the integrated fluorescence to that of a molecule with a known yield at the same wavelength. This photoinitiator generates radicals via intersystem crossing into the lowest triplet state,[18] which is likely to be the dominant pathway for nonradiative relaxation. We therefore assume that ϕ_2 is on the order of 0.99 with 800 nm excitation. Because the fluorescence quantum yield of Lucirin TPO-L is so low, as is the case with all efficient type I photoinitiators, it was not possible to determine σ_2 independently with a fluorescence-based method.[16,19]

To determine the polymerization action spectrum, $P_{th,fab}$ was measured as a function of excitation wavelength. A plot of the inverse of the square of the threshold power for fabrication is shown in Fig. 2, along with a linear absorption spectrum. While $A(\omega)$ tracks the red edge of the linear absorption spectrum, it rises above the linear spectrum on the blue edge of the absorption band. This is likely to be due to an increase in the two-photon absorption cross section relative to the single-photon cross section, as the radical quantum yield is generally believed to be independent of wave-
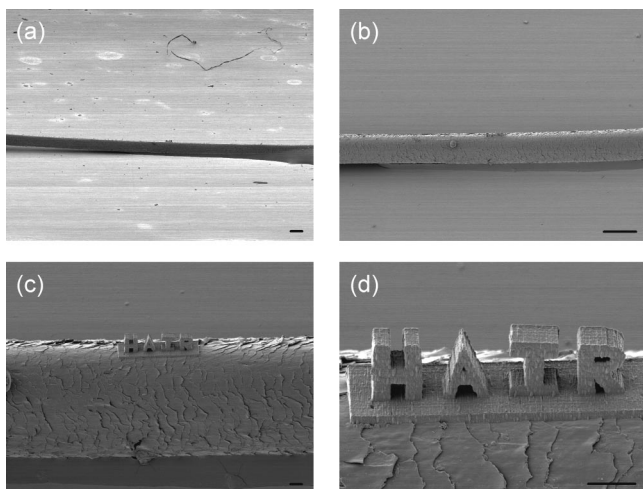

FIG. 3. (a)–(d) SEM images of a three-dimensional structure fabricated on top of a human hair at increasing magnification. Scale bars are 100 μm in (a) and (b) and 10 μm in (c) and (d).
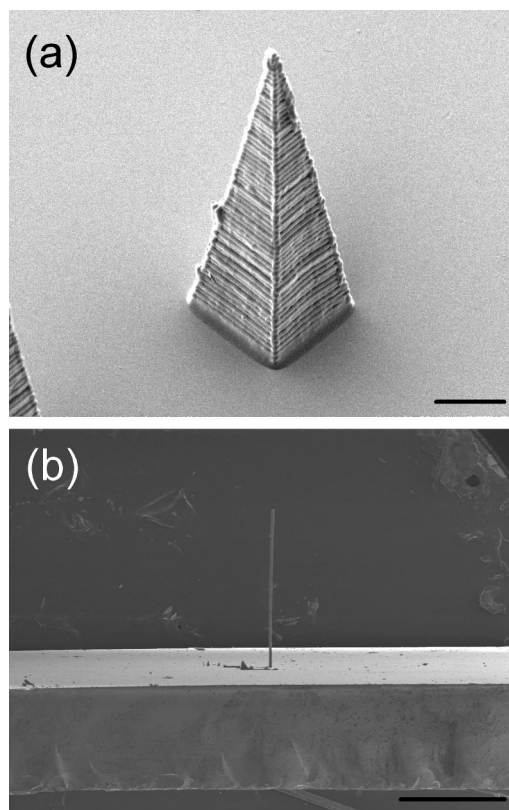

FIG. 4. SEM images demonstrating the structural integrity of structures created with MPP. Image (a) is a pyramid for which the exterior was fabricated with MPP and the interior was subsequently solidified without causing any change in the structure. The scale bar is 10 μm. Image (b) is a side view of a 1.5-mm tower that is 20 μm on each side; for comparison, the thick line at the bottom of the image is the side of the microscope slide on which the tower was fabricated. The scale bar is 1 mm.

length within a given absorption band. An independent measurement of σ_2 will be necessary to resolve this issue completely.

We conclude from Fig. 2 that Lucirin TPO-L initiates MPP most efficiently near a wavelength of 725 nm. However, MPP still occurs relatively efficiently and with a large dynamic range in the wavelength range in which most nontunable Ti:sapphire oscillators operate, near 800 nm. By 775 nm the MPP efficiency has reached more than half of its peak value.

IV. POLYMERIC STRUCTURES

Figure 3 shows scanning electron micrographs (SEMs) of different views of a three-dimensional structure that was fabricated on top of a human hair using MPP in order to demonstrate the lithographic resolution of this technique. The structure, and all of the following ones unless otherwise noted, was fabricated with a 1.3 NA oil-immersion objective. The power used was 2.3 mW and the lateral scan rate was 30 μm/sec. The hair is approximately 110 μm in diameter, which is more than an order of magnitude larger than the smallest dimensions of the polymerized features on the object, the narrowest of which have a dimension of 5 μm; some of the negative features, such as the gap in the letter A, are considerably smaller than this as well. Despite its small di-
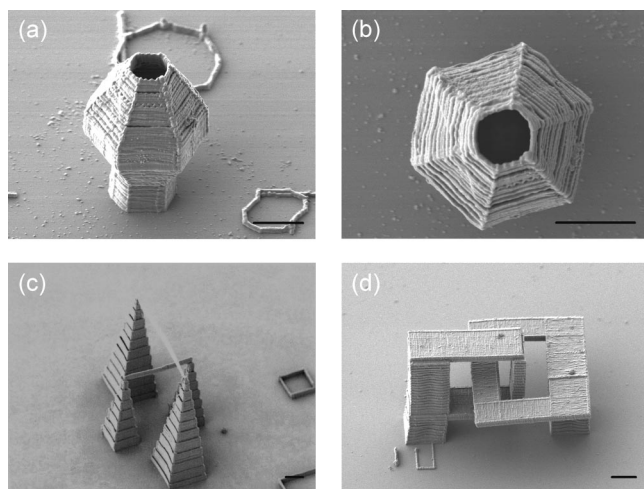
FIG. 5. SEM images of representative structures created with MPP that are not amenable to standard lithographic approaches. Images (a) and (b) show a hollow tower that is wider at intermediate heights than at the top or bottom. Image (c) shows two pairs of pyramids of different heights, with cables crossing between the pairs one over the other. Image (d) shows a pair of towers with interlocking rings. All scale bars are 10 μm.
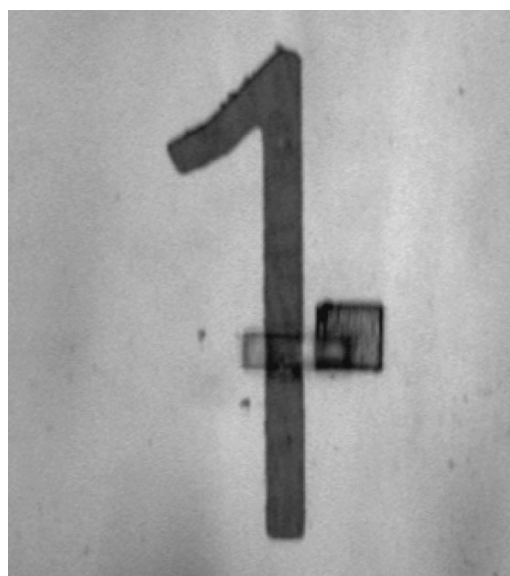

FIG. 6. Optical micrograph of a cantilever fabricated via MPP through which a number on a microscope reticle can be seen, demonstrating the high optical quality of the polymer.

mensions, the object shows excellent structural integrity. The lack of sagging or distortion of the structure is indicative of the excellent mechanical properties of the polymer, and the straightness of the vertical edges near the base demonstrates that the resin does not shrink significantly during polymerization. Indeed, elastic measurements that will be presented elsewhere show that the polymer has a bulk modulus on the order of a GPa.

Additional structures that are indicative of the mechanical strength of the polymer are shown in Fig. 4. Figure 4(a) shows a pyramid that was created at a power of 2.5 mW and a scan rate of 10 μm/sec. In this case only the exterior of the object was created with MPP, and after washing the unexposed resin inside the object was cured with an ultraviolet lamp. The postcuring procedure caused no visible change in the shape of the pyramid, despite the fact that in the bulk the resin does shrink by a few percent upon polymerization. Thus, the polymerized shell of the pyramid had enough structural rigidity to withstand any tension created in the postcuring process.

Figure 4(b) is a scanning-electron micrograph of a tower that is 1.5 mm tall and only 20 μm on each side. This structure was created with a 0.3 NA objective at a power of 30 mW. The 75:1:1 aspect ratio of this object could not have been achieved with any standard lithographic technique, and further demonstrates the superb mechanical strength of this polymer formulation. The only special care that was taken in the fabrication of this tower was to hold the substrate upside down during the washing process to help prevent drops of solvent from bending the tower down. The limiting factor in the height of this object was the working distance of the objective, and structures with even higher aspect ratios would presumably also be stable.

Shown in Fig. 5 are SEM images of representative structures that could not be created with standard lithographic techniques but are straightforward to fabricate using MPP.

Figures 5(a) and 5(b) show different views of a hollow tower that is broader in its middle than at its top or bottom. The tower was fabricated using a power of 2.0 mW at a scan rate of 20 μm/sec, and gives another example of the excellent structural integrity of the polymer.

Figure 5(c) is a scanning electron microscopy image of two pairs of towers of different heights, with a cable running between the taller towers and another cable running beneath it between the shorter towers. The structure was fabricated at a power of 5.0 mW with a scan rate of 10 μm/sec. This structure highlights the potential for the creation of three-dimensional circuitry if MPP were combined with selective metallization. Figure 5(d) is a SEM image of two interlocking rings on posts. This structure was created at a power of 3.4 mW with a scan rate of 20 μm/sec, and demonstrates that structures with arbitrarily complex topologies can be created readily using MPP.

Lastly, we consider the optical properties of structures made with the resin described here. Figure 6 shows an optical micrograph of a cantilever that was fabricated on top of a microscope reticle. The cantilever arm is approximately 15 μm above the number on the reticle, which has a stroke width of 25 μm. The image was obtained in air, and demonstrates the high optical quality of the polymerized resin. Some amount of surface roughness of the polymer can be seen in this image, but any roughness can be reduced significantly by fabricating with a shorter distance between adjacent lines.

V. CONCLUSIONS

In this paper we have described and characterized a prepolymer resin with favorable properties for MPP of complex three-dimensional structures. The resin is comprised of readily available components, and its preparation is straightforward. This resin allows for the fabrication of complex three-dimensional structures with high structural rigidity us-

ing only a small fraction of the output power of a Ti:sapphire oscillator. We are currently pursuing the use of this material in the fabrication of functional microdevices via MPP.

ACKNOWLEDGMENTS

[1] C. J. R. Sheppard and R. Kompfner, Appl. Opt. **17**, 2879 (1978).

[2] W. Denk, J. H. Strickler, and W. Webb, Science **248**, 73 (1990).

[3] Patrik R. Callis, Annu. Rev. Phys. Chem. **48**, 271 (1997).

[4] Shoji Maruo, Osamu Nakamura, and Satoshi Kawata, Opt. Lett. **22**, 132 (1997).

[5] Shoji Maruo and Satoshi Kawata, J. Microelectromech. Syst. **7**, 411 (1998).

[6] S. Maruo, K. Ikuta, and H. Korogi in *Proceedings of the 14th IEEE International Conference on Micro Electro Mechanical Systems* (IEEE, Piscataway, NJ, 2001). p. 594.

[7] G. Witzgall, R. Vrijen, E. Yablonovitch, V. Doan, and B. J. Schwartz, Opt. Lett. **23**, 1745 (1998).

[8] H. B. Sun, T. Tanaka, K. Takada, and S. Kawata, Appl. Phys. Lett. **79**, 1411 (2001).

[9] S. Kawata, H. B. Sun, T. Tanaka, and K. Takada, Nature (London) **412**, 697 (2001).

[10] H. B. Sun, T. Tanaka, and S. Kawata, Appl. Phys. Lett. **80**, 3673 (2002).

[11] Kevin D. Belfield, Xiaobin Ren, Eric W. Van Stryland, David J. Hagan, Vladislav Dubikovsky, and Edward J. Miesak, J. Am. Chem. Soc. **122**, 1217 (2000).

[12] Tommaso Baldacchini, Huzhen Chen, Richard A. Farrer, Michael J. R. Previte, Joel Moser, Michael J. Naughton, and John T. Fourkas, in *Commercial and Biomedical Applications of Ultrafast Lasers*, edited by Glenn S. Edwards *et al.* (SPIE, Bellingham, WA, 2002), p. 136.

[13] T. Baldacchini, R. A. Farrer, J. Moser, J. T. Fourkas, and M. J. Naughton, Synth. Met. **135**, 11 (2003).

[14] J. Serbin, A. Egbert, A. Ostendorf, B. N. Chichkov, R. Houbertz, G. Domann, J. Schulz, C. Cronauer, L. Frohlich, and M. Popall, Opt. Lett. **28**, 301 (2003).

[15] Brian H. Cumpston, Sundaravel P. Ananthavel, Stephen Barlow, Daniel L. Dyer, Jeffery E. Ehrlich, Lael L. Erskine, Ahmed A. Heikal, Stephen M. Kuebler, I.-Y. Sandy Lee, Dianne McCord-Maughon, Jinqui Qin, Harald Rockel, Mariacristina Rumi, Xiang-Li Wu, Seth R. Marder, and Joseph W. Perry, Nature (London) **398**, 51 (1999).

[16] Paul J. Campagnola, David M. Delguidice, Gary A. Epling, Kurt D. Hoffacker, Amy R. Howell, Jonathan D. Pitts, and Steven L. Goodman, Macromolecules **33**, 1511 (2000).

[17] Shoji Maruo and Koji Ikuta, Appl. Phys. Lett. **76**, 2656 (2000).

[18] C. S. Colley, D. C. Grills, N. A. Besley, S. Jockusch, P. Matousek, A. W. Parker, M. Towrie, N. J. Turro, P. M. W. Gill, and M. W. George, J. Am. Chem. Soc. **124**, 14 952 (2002).

[19] Chris Xu and Watt W. Webb, J. Opt. Soc. Am. B **13**, 481 (1996).